10 Yokoyama T, Vaca L, Rossen RD, Durante W, Hazarika P, Mann DL: Cellular basis for the negative inotropic effects of tumor necrosis factor-alpha in the adult mammalian heart. *J Clin Invest* 1993; 92: 2303 – 2312.
11 Lodge-Patch I: The aging of cardiac infarcts, and its influence on cardiac rupture. *Br Heart J* 1951; 13: 37 – 42.
12 Wong SC, Fukuchi M, Melnyk P, Rodger I, Giaid A: Induction of cyclooxygenase-2 and activation of nuclear factor-κB in myocardium of patients with congestive heart failure. *Circulation* 1998; 98: 100 – 103.
13 Pischon T, Girman CJ, Hotamisligil GS, Rifai N, Hu FB, Rimm EB: Plasma adiponectin levels and risk of myocardial infarction in men. *JAMA* 2004; 291: 1730 – 1737.
14 Furuhashi M, Ura N, Moniwa N, Shinshi Y, Kouzu H, Nishihara M, *et al*: Possible impairment of transcardiac utilization of adiponectin in patients with type 2 diabetes. *Diabetes Care* 2004; 27: 2217 – 2221.
15 Ishikawa Y, Akasaka Y, Ishii T, Yoda-Murakami M, Choi-Miura NH, Tomita M, *et al*: Changes in the distribution pattern of gelatin-binding protein of 28 kDa (adiponectin) in myocardial remodelling after ischaemic injury. *Histopathology* 2003; 42: 43 – 52.
16 Yoda-Murakami M, Taniguchi M, Takahashi K, Kawamata S, Saito K, Choi-Miura NH, *et al:* Changes in expression of GBP28/adiponectin in carbon tetrachloride-administrated mouse liver. *Biochem Biophys Res Commun* 2001; 285: 372 – 377.
17 Yamauchi T, Kamon J, Ito Y, Tsuchida A, Yokomizo T, Kita S, *et al*: Cloning of adiponectin receptors that mediate antidiabetic metabolic effects. *Nature* 2003; 423: 762 – 769.

Address for correspondence
Dr T Kanda
Department of General Medicine, Kanazawa Medical University, 1-1 Daigaku, Uchinada-machi, Kahoku-gun, Ishikawa, 920-0293, Japan.
E-mail: kandat@kanazawa-med.ac.jp

Osteoclast-like cells express receptor activity modifying protein 2: application of laser capture microdissection

M Nakamura[1], S Morimoto[2], Q Yang[1,4], T Hisamatsu[1], N Hanai[3], Y Nakamura[1], I Mori[1] and K Kakudo[1]

[1]Second Department of Pathology, Wakayama Medical University, Kimiidera 811-1, Wakayama City, Wakayama, 641-0012, Japan

[2]Department of Geriatric Medicine, Kanazawa Medical University, Uchinada 1-1, Ishikawa, Ishikawa, 920-0290, Japan

[3]Department of Pediatrics, Wakayama Medical University, Kimiidera 811-1, Wakayama City, Wakayama, 641-0012, Japan

[4]The Cancer Institute of New Jersey, UMDNJ-Robert Wood Johnson Medical School, 195 Little Albany Street, New Brunswick, New Jersey 08903, USA

(Requests for offprints should be addressed to M Nakamura; Email: marumisa@wakayama-med.ac.jp)

Abstract

Receptor activity modifying proteins (RAMPs) act as receptor modulators that determine the ligand specificity of receptors for the calcitonin (CT) family. The purpose of this study was to analyze the expression of RAMPs in osteoclast-like cells using the laser capture microdissection (LCM) technique. Mouse bone marrow and spleen cells were co-cultured on a film designed for LCM. After 10 days, 250 osteoclast-like cells were captured using the LCM system. Total RNA from these cells was used to synthesize cDNA and RT-PCR analysis was performed. Osteoclast-like cells expressed CT receptor (CTR), CT receptor-like receptor (CRLR) and RAMP2, but did not express RAMP1 or RAMP3. These results indicated (1) that a pure population of osteoclast-like cells can be prepared by LCM and gene expression of this population can be analyzed by RT-PCR and (2) that RT-PCR shows that osteoclast-like cells express RAMP2, CTR and CRLR, suggesting the potential for adrenomedullin binding to osteoclast-like cells. This is the first report that osteoclast-like cells express RAMP2.

Journal of Molecular Endocrinology (2005) **34**, 257–261

Introduction

The calcitonin (CT) family of peptides comprises five known members: CT, amylin (AMY), two CT gene-related peptides (CGRP1 and CGRP2) and adrenomedullin (ADM). Receptor activity modifying proteins (RAMPs) comprise a family of accessory proteins for G protein-coupled receptors, three of which act as receptor modulators that determine the ligand specificity of receptors for CT family members. CT receptor-like receptor (CRLR) has been shown to form a high affinity receptor for CGRP, when associated with RAMP1, or, when associated with RAMP2 or RAMP3, to specifically bind ADM (McLatchie *et al.* 1998, Sexton *et al.* 2001). RAMPs are type I transmembrane proteins that share ~30% amino acid identity and a common predicted topology, with short cytoplasmic C termini, one transmembrane domain and large extracellular N termini that are responsible for the specificity (McLatchie *et al.* 1998, Fraser *et al.* 1999). More recently, CT receptor (CTR) was demonstrated to form heterodimeric complexes with RAMP. CTR/RAMP1 and CTR/RAMP3 heterodimers exhibited the pharmacological profiles of receptors specific for AMY (Christopoulos *et al.* 1999, Muff *et al.* 1999, Sexton *et al.* 2001).

There is significant interest in analyzing gene expression of distinct cell populations. Heterogeneous populations of cells within tissues of various types possess correspondingly different patterns of gene expression, and these cell types must be separated from one another for accurate assessment of gene expression. Tong *et al.* (1994) has reported that a microisolation system using a micromanupilator tool was applied for mRNA phenotyping of a blood cell lineage. Laser capture microdissection (LCM) is a particularly useful tool for recovering small cell samples and even enables the collection of individual cells from tissue sections (Emmert-Buck *et al.* 1996). This method facilitates the separation of histologically distinct cells so that proteins, DNA or RNA from these cells can be analyzed in isolation from the surrounding cells (Bonner *et al.* 1997). Osteoclasts act centrally in the remodeling of bone in normal and diseased states. Nonetheless, because of their low numbers within bone, cell culture model systems have been increasingly used to investigate the biochemical functions of osteoclasts (Udagawa *et al.*1989, Nakamura *et al.* 1998). However, because of their heterogeneity and adherence to the plate in such systems, there has been difficulty and controversy in analyzing these cell types. Thus, a more sensitive isolation method for osteoclasts is needed.

Journal of Molecular Endocrinology (2005) **34**, 257–261
0952–5041/05/034–257 *Printed in Great Britain*

DOI: 10.1677/jme.1.01652
Online version via http://www.endocrinology-journals.org

To address this problem, we used LCM techniques to isolate a pure population of osteoclast-like cells. We then analyzed RAMP gene expression in microdissected osteoclast-like cells using RT-PCR.

Materials and methods

An *in vitro* osteoclast model

Osteoclast differentiation *in vitro* was induced using the technique described by Udagawa *et al.* (1989). Both bone marrow cells and spleen cells were obtained from 10- to 14-week-old male C57BL/6 mice (Charles River, Sagamihara, Japan). The bone marrow cells were collected from tibiae and femora. Splenic tissue was cut with scissors and dispersed by pipetting, then the spleen cells were collected by centrifugation at 1000 r.p.m. for 5 min at 4 °C. Bone marrow cells were co-cultured with spleen cells (2×10^6 cells/ml for each cell type) on a film produced for use in LCM (Matsunami Glass Co., Osaka, Japan) for 10 days at 37 °C in a humidified atmosphere of 5% CO_2. Cultures were fed with α-modified Eagle's medium supplemented with penicillin and streptomycin, 10% fetal calf serum (Hyclone, Logan, UT, USA) and 10^{-8} M $1,25(OH)_2$ D_3 (Calbiochem-Novabiochem Co., San Diego, CA, USA). Multinucleated osteoclast-like cells were then isolated using LCM. All the animal experimental procedures were approved by the Animal Care and Use Committee of Wakayama Medical University (Wakayama, Japan).

LCM of samples

Before LCM, cells were fixed in ethanol for 1 min and stained for 3 min with filtered hematoxylin. They were then washed with sterilized water and air-dried for 10 min. LCM of cultured osteoclast-like cells was performed using the Application Solutions Laser Microdissection System (Leica Microsystems Co., Tokyo, Japan) according to the manufacturer's instructions.

RNA isolation

Total RNA was extracted from 250 LCM-captured cells and 250 spleen cells. The spleen cells used for RNA extraction were from an aliquot of those prepared for the co-culture system. Total RNA extraction was performed using TRIzol LS Reagent (Invitrogen Life Technologies Co., Carlsbad, CA, USA) as described by the manufacturer. Briefly, 170 μl TRIzol reagent was added to a tube containing LCM cells and this was incubated for 5 min at room temperature. Forty microliters of chloroform were then added and the tube was incubated at room temperature for a further 15 min. The samples were then centrifuged at 12 000 ***g*** for 15 min. The aqueous phase was transferred to a ne tube and isopropyl alcohol was added followed b centrifugation at 12 000 ***g*** for 10 min. The RN precipitate was washed with 70% ethanol and dissolve in 20 μl sterilized water.

RT-PCR

The SUPERSCRIP One-Step RT-PCR with PLATI NUM *Taq* (Invitrogen Life Technologies Co.) was use to synthesize cDNA and PCR was performed a described by the manufacturer. The nucleic aci sequences of primers used for RT-PCR are shown ir Table 1. RT-PCR reactions were initially performed ir a 25 μl reaction volume containing 1 μl of each prime (at 100 ng/μl) and 3 μl RNA as template. The reaction were run at 55 °C for 30 min (cDNA synthesis) anc 94 °C for 2 min (pre-denaturation), followed by 45 cycle of 94 °C for 30 s (denaturation), 53 °C for 30 s (annealing) and 72 °C for 30 s (extension), followec by 7 min at 72 °C (final extension). To increase the detection capacity, we performed a second round o PCR. The second-round PCR reactions were carried ou using Taq polymerase (Perkin-Elmer-Cetus, Norwalk CT, USA) with 8 μl RT-PCR products as template (fina 25 μl reaction mixture) under the following conditions 35 cycles of 95 °C for 30 s, 55 °C for 30 s and 72 °C fo 30 s. In the second-round PCR, CTR was amplifiec using 2nd sense and anti-sense primers (Table 1). The primers of CRLR, RAMP1, 2, 3, alkaline phosphatase (ALP) and β-actin for the second-round PCR were the same primers as those used in the initial RT-PCR. The samples were electrophoresed in 3% agarose gels anc stained with ethidium bromide.

Results and discussion

We have developed a rapid and precise method for the isolation of pure populations of osteoclast-like cells using LCM. Figure 1 illustrates two osteoclast-like cells before and after LCM. Two hundred and fifty cells with > three nuclei each were isolated. Total RNA was extracted and RT-PCR was used to analyze multiple gene expressions. Figure 2 shows the RT-PCR results for CTR, RAMP1, 2 and 3, CRLR and β-actin. The predicted sizes were clearly visualized by ethidium bromide staining. RT-PCR results showed that the ubiquitous gene, β-actin, was amplified from both spleen and osteoclast-like cells, whereas CTR mRNA was amplified from osteoclast-like cells alone. RAMP1 and RAMP3 mRNAs were amplified from spleen cells alone. RAMP2 and CRLR mRNAs were amplified from both types of cells.

In the present study, we were able to isolate a pure population of osteoclast-like cells and detect a series of gene expressions. Two hundred and fifty cells were

Table 1 Oligonucleotide sequences used for PCR

Target	Sequence	Size
CTR	1st sense, 5′-GTCTTGCAACTACTTCTGGATGC-3′ 1st antisense, 5′-AAGAAGAAGTTGACCACCAGAGC-3′ 2nd sense, 5′-GTCTTGCAACTACTTCTGGATGC-3′ 2nd antisense, 5′-GAAGATAGTACCAGCGTAGGC-3′	255 bp (Inoue *et al.* 1999) 104 bp (U18542*)
RAMP1	Sense, 5′-CACCATCTCTTCATGGTCACTG-3′ Antisense, 5′-CAATCGTGTGCGCCACGTGC-3′	187 bp (AJ250489)
RAMP2	Sense, 5′-TGGATCTCGGCTTGGTGTGAC-3′ Antisense, 5′-GCAAGGTAGGACATGTGTTTCG-3′	217 bp (AJ250490)
RAMP3	Sense, 5′-TTGTGGTGAGTGTGCCCAGG-3′ Antisense, 5′-CCCATGATGTTGGTCTCCATC-3′	189 bp (AJ250491)
CRLR	Sense, 5′-TGTAATAACAGCACGCATGAG-3′ Antisense, 5′-GTTATTGGCCACTGCCGTGA-3′	225 bp (AF146525)
ALP	Sense, 5′-ATCGGGACTGGTACTCGGATAA-3′ Antisense, 5′-ATCAGTTCTGTTCTTCGGGTAC-3′	152 bp (NM007431)
β-Actin	Sense, 5′-GTGGGCCGGTCTAGGCACCA-3′ Antisense, 5′-GGTTGGCCTTAGGGTTCAG-3′	246 bp (Flores-Delgado *et al.* 1998)

*Accession number of GeneBank.
ALP, alkaline phosphatase.

used for RNA extraction and cDNA synthesis. Three microliters of the 20 μl cDNA solution was successful for each gene amplification. Approximately 40 cells were therefore used for RT-PCR analysis. Naot *et al.* (2001) have reported that osteoclastic cells such as primary osteoblasts and UMR 106-06 cells expressed all three types of RAMP analyzed using RT-PCR. A very high expression of mRNA for RAMP2 was detected in those cells, compared with those for RAMP1 and RAMP3. Previous studies showed that osteoblast but not osteoclast cells express ALP (Tong *et al.* 1994). To exclude the possibility of osteoblast contamination, we investigated ALP mRNA expression in the microdissected osteoclast-like cells. The result showed that no ALP mRNA was detectable (Fig. 3), which supported the idea that RAMP2 was amplified from osteoclast-like cells. Thus, LCM is a useful technique for isolation of small cell samples, and our strategy might be extended to other procedures, such as quantitative RT-PCR to measure mRNA levels in the osteoclast. The bone marrow macrophages are the precursors of osteoclasts; it will be interesting to compare gene expression between osteoclasts and bone marrow macrophages. Immunostaining of the Fc receptor, C3 receptor or vitamin D receptor will help to distinguish those cell types in our co-culture system. However, in order to perform RNA

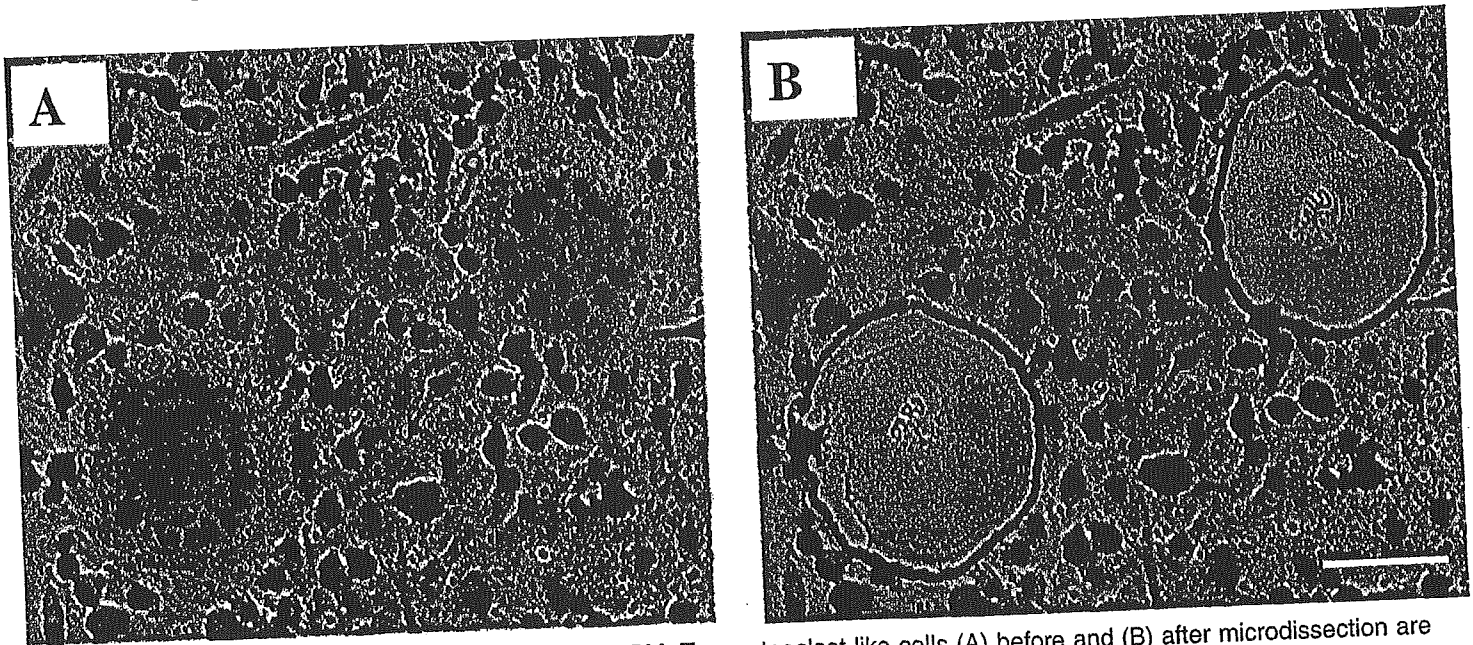

Figure 1 Osteoclast-like cells were isolated by using LCM. Two osteoclast-like cells (A) before and (B) after microdissection are shown. Stained by hematoxylin; bar denotes 50 μm.

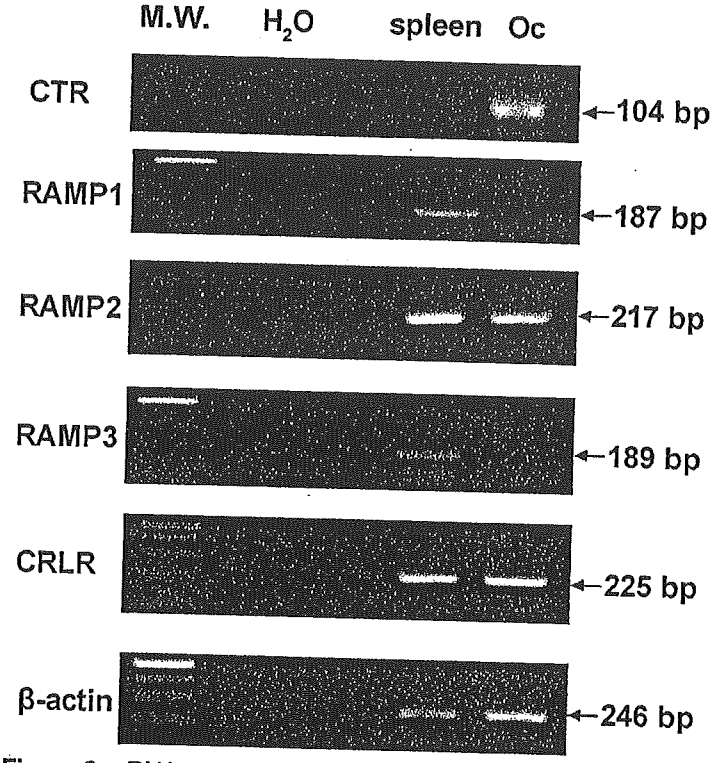

Figure 2 mRNA expression of various genes in spleen and osteoclast-like cells. Total RNA was extracted from microdissected osteoclast-like cells and spleen cells, RT-PCR was carried out to analyze the gene expression. β-actin served as the positive control. The products were electrophoresed in 3% agarose gels and stained with ethidium bromide. RAMP1, RAMP2, RAMP3 and CRLR were detected in spleen cells. M.W., molecular weight markers; H_2O, H_2O as template served as negative control; spleen, using RNA from spleen as template; Oc, using RNA from osteoclast-like cells from LCM as template.

analysis after immunostaining, further efforts should be made to modify the conventional staining protocol to protect RNA from degradation.

Our findings that osteoclast-like cells expressed RAMP2 and CRLR as well as CTR provide the first evidence that osteoclasts express RAMP2. These results suggest that osteoclasts may have the ability to bind ADM through the CRLR/RAMP2 heterodimer. ADM is a 52 amino acid peptide first described in a human phaeochromocytoma but subsequently found to be present in many tissues, including the vascular system and bone tissue (Kitamura *et al.* 1993). Naot *et al.* (2001) has suggested that ADM is mitogenic to osteoblasts, raising the possiblity that ADM is a local regulator of bone growth; however, the action of ADM or RAMP on the osteoclast is not clear. It has been reported that bone abnormalities were observed in both CTR +/− and AMY +/− mice, thereby ruling out the possibility that AMY uses CTR to inhibit osteoclastogenesis *in vivo* (Dacquin *et al.* 2004).

In summary, we have demonstrated that LCM is a useful solution for osteoclast research. We found that osteoclast-like cells expressed mRNAs for CTR, CRLR and RAMP2 but not RAMP1 or RAMP3; RAMP2 may therefore play an important role in osteoclast function. Further study is needed to elucidate the role of RAMP2 and its relationship to the CT family of receptors.

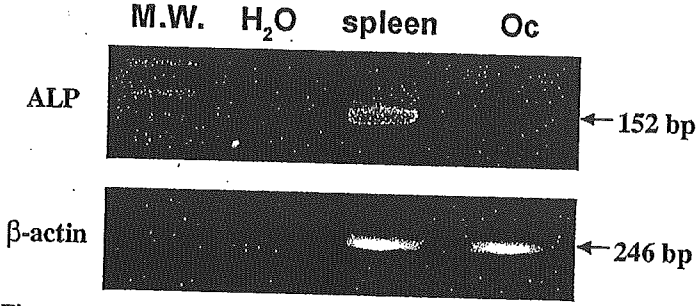

Figure 3 RT-PCR analysis of ALP expression. ALP expression was detected in spleen cells but not in osteoclast-like cells. M.W., molecular weight markers; H_2O, RT-PCR products using H_2O as template; spleen, using RNA from spleen as template; Oc, using RNA from osteoclast-like cells from LCM as template.

Acknowledgements

We thank Dr Yomekazu Sakamoto (Matsunami Glass Ind., Ltd) and Dr Hirotoshi Utsunomiya (Wakayama Medical University) for their technical advice on the LCM methodology. This research was supported by funding from the Health Sciences Research Grants 'Comprehensive Research on Aging and Health' (13030201) from the Ministry of Health, Labor and Welfare of Japan. The authors are grateful to Dr Danielle Frikker (The Cancer Institute of New Jersey) for critical review of our manuscript. The authors declare that there is no conflict of interest that would prejudice the impartiality of this scientific work.

References

Bonner RF, Emmert-Buck MR, Cole K, Pohida T, Chuaqui R, Goldstein S & Liotta L 1997 Laser capture microdissection: molecular analysis of tissue. *Science* **278** 1481–1483.

Christopoulos G, Perry KJ, Morfis M, Tilakaratne N, Gao Y, Fraser NJ, Main MJ, Foord SM & Sexton PM 1999 Multiple amylin receptors arise from receptor activity-modifying protein interaction with the calcitonin receptor gene product. *Molecular Pharmacology* **56** 235–242.

Dacquin R, Davey RA, Laplace C, Levasseur R, Morris HA, Goldring SR, Gebre-Medhin S, Galson DL, Zajac JD & Karsenty G 2004 Amylin inhibits bone resorption while the calcitonin receptor controls bone formation *in vivo*. *Journal of Cell Biology* **164** 509–514.

Emmert-Buck MR, Bonner RF, Smith PD, Chaqui RF, Zhunag Z, Goldstien SR, Weiss RA & Liota L 1996 Laser capture microdissection. *Science* **274** 998–1001.

Flores-Delgado G, Bringas P & Warburton D 1998 Laminin 2 attachment selects myofibroblasts from fetal mouse lung. *American Journal of Physiology* **275** L622–L630.

Fraser NJ, Wise A, Brown J, McLatchie LM, Main MJ & Foord SM 1999 The amino terminus of receptor activity modifying proteins is a critical determinant of glycosylation state and ligand binding of calcitonin receptor-like receptor. *Molecular Pharmacology* **55** 1054–1059.

Inoue D, Shih C, Galson DL, Goldring SR, Horne WC & Baron R 1999 Calcitonin-dependent down-regulation of the mouse C1a calcitonin receptor in cells of the osteoclast lineage involves a transcriptional mechanism. *Endocrinology* **140** 1060–1080.

Kitamura K, Kangawa K, Kawamoto M, Ichiki Y, Nakamura S, Matsuo H & Eto T 1993 Adrenomedullin: a novel hypotensive peptide isolated from human pheochromocytoma. *Biochemical and Biophysical Research Communications* **192** 553–560.

McLatchie LM, Fraser NJ, Main MJ, Wise A, Brown J, Thompson N, Solari R, Lee MG & Foord SM 1998 RAMPs regulated the transport and ligand specificity of the calcitonin-receptor-like receptor. *Nature* **393** 333–339.

Muff R, Buhlmann N, Fischer JA & Born W 1999 An amylin receptor is revealed following co-transfection of a calcitonin receptor with receptor activity modifying proteins-1 or -3. *Endocrinology* **140** 2924–2927.

Nakamura I, Jimi E, Duong LT, Sasaki T, Takahashi N, Rodan GA & Suda T 1998 Tyrosine phosphorylation of p130 Cas is involved in actin organization in osteoclasts. *Journal of Biological Chemistry* **273** 11144–11149.

Naot D, Callon KE, Grey A, Cooper GJ, Reid IR & Cornish 2001 A potential role for adrenomedullin as a local regulator of bone growth. *Endocrinology* **142** 1849–1857.

Sexton PM, Albiston A, Morfis M & Tilakaratne N 2001 Receptor activity modifying proteins. *Cellular Signalling* **13** 73–83.

Tong HS, Sakai DD, Sims SM, Dixon SJ, Yamin M, Goldring SR, Snead ML & Minkin C 1994 Murine osteoclasts and spleen cell polykaryons are distinguished by mRNA phenotyping. *Journal of Bone and Mineral Research* **9** 577–584.

Udagawa N, Takahashi N, Akatsu T, Sasaki T, Yamaguchi A, Kodama H, Martin TJ & Suda T 1989 The bone marrow-derived stromal cell lines MC3T3- G2/PA6 and ST2 support osteoclast-like cell differentiation in cocultures with mouse spleen cells. *Endocrinology* **125** 1805–1813.

Received 22 October 2004
Accepted 1 November 2004

Erratum

The authors apologize for an error in the paper by Li Chen, Jinsong Zhu, Guoqiang Sun and Alexander S Raikhel which appeared in the December 2004 issue of *Journal of Molecular Endocrinology* **33** 743–761, titled 'The early gene *Broad* is involved in the ecdysteroid hierarchy governing vitellogenesis of the mosquito *Aedes aegypti*'.

Page 757 read:
and JH blocks their appearance in larval *Manduca* (Zhou & Riddiford 2002).

When it should have read:
and JH blocks their appearance in larval *Manduca* (Zhou *et al.*, 1998).

Page 759 read:
misexpression of Z1 causes the reappearance of a pup cuticle gene *Edg78E* and suppresses a larval cuticle ger *Lcp65A-b*.

When it should have read:
misexpression of Z1 causes the reappearance of a pup: cuticle gene *Edg78E* and suppresses a larval cuticle gen *Lcp65A-b* (Zhou & Riddiford, 2002).

Journal of Molecular Endocrinology (2005) **34**, 262
0952–5041/05/034–262

DOI: 10.1677/jme.1.01531
Online version via http://www.endocrinology-journals.o

Volume 97, Number 2, July 22, 2005
ISSN 0009-7330
http://circres.ahajournals.org

American Heart Association®
Learn and Live℠

Circulation Research

JOURNAL OF THE AMERICAN HEART ASSOCIATION

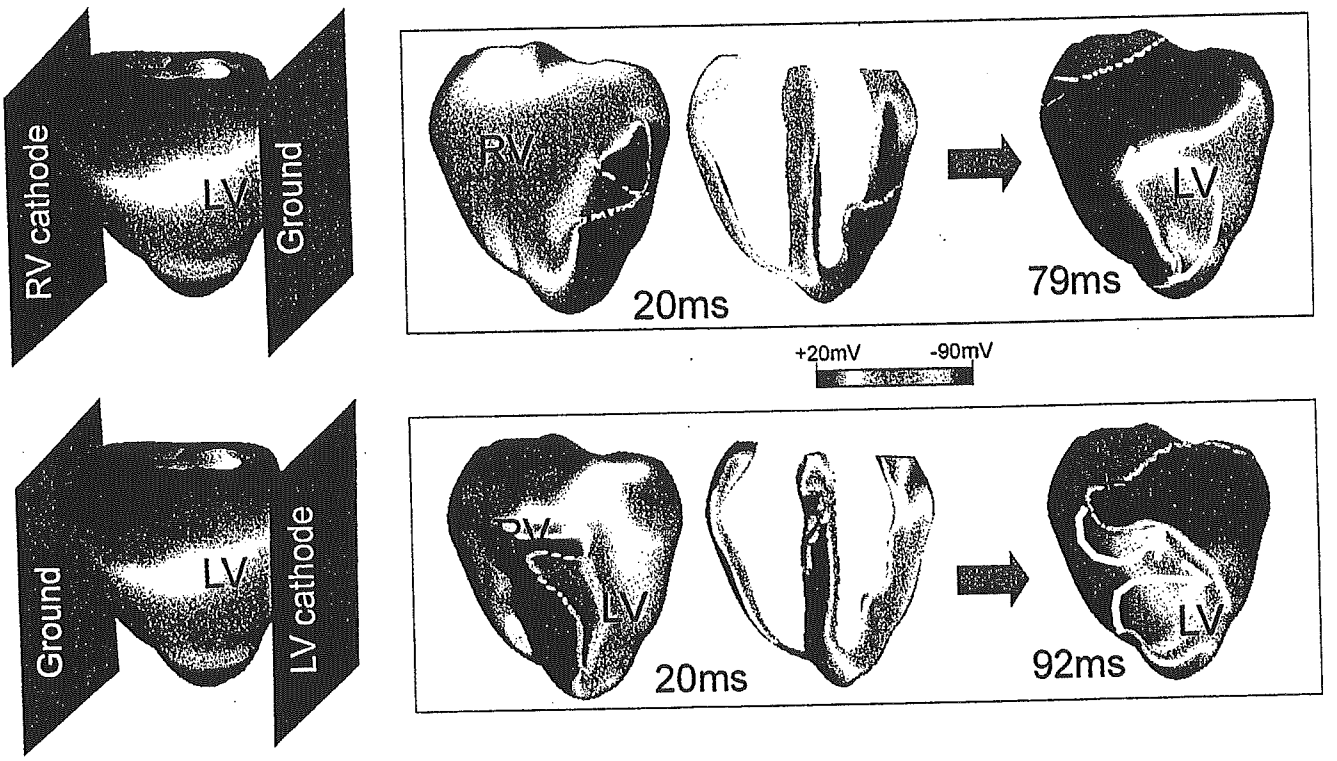

Abstracts

Second Annual Symposium of the American Heart Association Council on Basic Cardiovascular Sciences

Targeting Heart Failure—New Science, New Tools, New Strategies

July 24–27, 2005
Keystone Conference Center
Keystone, CO

Sponsored by the American Heart Association Council on Basic Cardiovascular Sciences
Co-sponsored by the American Heart Association Interdisciplinary Working Group on Functional Genomics & Translational Biology and the National Heart, Lung, and Blood Institute

Heart failure remains a leading cause of death in the adult population, affecting more than 5 million individuals in the United States alone. This second annual meeting of the American Heart Association Council on Basic Cardiovascular Sciences highlights new research that has aimed at expanding our knowledge of the underlying mechanisms, diagnostic approaches, and therapeutic strategies to treat this common disorder. The meeting features both invited presentations and poster abstract presentations, with participants from 21 different countries.

Abstracts for the poster presentations are provided in this special online supplement.

(*Circ Res.* 2005;97:199)

Circulation Research is available at http://circres.ahajournals.org

following I/R in hearts with defective TLR4. To determine the role of ROS in TLR4-mediated inflammatory response, hearts were stimulated with hydrogen peroxide (0.25 mM/L). While hydrogen peroxide induced the production of MIP-2 and TNF-alpha in hearts isolated from control mice, its effects were greatly attenuated in hearts with defective TLR4. Further experiments using isolated macrophages confirmed that hydrogen peroxide induces NF-kappaB intranuclear translocation and inflammatory mediator production in a TLR4-dependent manner. We conclude that TLR4 signaling plays a novel role in the regulation of post-ischemic cardiac inflammatory response and that ROS may mediate this response through activation of TLR4.

X. Meng, None; **L. Ao**, None; **J. Cha**, None; **M. Wang**, None; **D.A. Fullerton**, None.

P 98

Role of Dual-Specificity Phosphatases in the Heart as Revealed by Gene Targeting

Orlando F Bueno, Robert A Kaiser, Jian Xu, Benjamin J Wilkins, Jeffery D Molkentin, Children's Hosp Med Ctr, Cincinnati, OH

The mitogen-activated protein kinases (MAPK) have been shown to participate in diverse biological processes in the heart including cardiac hypertrophy, myocyte survival, and apoptosis. MAPKs are tightly regulated through the addition or removal of phosphate groups in threonine and tyrosine residues located in the activation loop domain. Inactivation of MAPKs is controlled by removal of these phosphate groups and is mediated through a family of proteins known as dual-specificity phosphatases (DSPs), which have a high degree of specificity for individual MAPK substrates. DSPs directly bind to their MAPK substrate and remove phosphate groups from both threonine and tyrosine residues located in the activation loop domain, allowing MAPKs to be recycled. The potential role of the downstream counter-acting DSPs has not been explored in the heart. Therefore, in order to evaluate the function of DSPs in the heart as well as the consequences of increased MAPK signaling, we have systematically inactivated by gene-targeting several of the most critical and heart-expressed counter-acting DSPs including, MKP-1, MKP-2 and MKP-5. This approach will provide the first "physiologic" assessment of sustained and/or prolonged MAPK activation and its consequences on the heart. Initial observations show that DSP-targeted mice display an overall increased MAPK activation in the heart following agonist and pressure overload stimulation. Moreover, analysis of MKP-1-/- x MKP-2-/- double mutant mice showed a significant increase in cardiac hypertrophy following chronic isoproterenol infusion and myocardial infarction. However, these double mutant mice subjected to chronic angiotensin II / phenylephrine infusion or 14 days of pressure overload induced by TAC did not show any alteration in the hypertrophic response when compared with wild-type animals. These preliminary results suggest that in DSP-deficient mice, the nature of the hypertrophic stimulus will determine the levels of activity in each of the MAPK branches and eventually establish the resulting phenotype.

O.F. Bueno, None; **R.A. Kaiser**, None; **J. Xu**, None; **B.J. Wilkins**, None; **J.D. Molkentin**, None.

P 99

Genome-Wide Expression Profiling of NFAT Transcriptional Activity in a Ventricular Muscle Cell Line

Meriem Bourajjaj, Anne-Sophie Armand, Hubrecht Lab, Utrecht, The Netherlands; Rhonda Bassel-Duby, Eric N Olson, Univ of Texas Southwestern Med Ctr, Dallas, TX; Leon J De Windt, Hubrecht Lab, Utrecht, The Netherlands

Cardiac hypertrophy is dependent upon activation of calcineurin-Nuclear Factor of Activated T cells (NFAT) signaling, but limited information is available on the nature and number of downstream NFAT target genes. Recently, cell lines were isolated from ventricular sarcomas from juvenile transgenic mice harboring a Nkx2.5-floxed SV40 T antigen (TAg) construct. NKL-TAg cells were isolated from sarcomas, which actively proliferate, and withdraw from the cell cycle and adopt a cardiac muscle cell fate upon Cre mediated loxP excision of the SV40 TAg (Rybkin et al. J Biol Chem 2003). We established a cellular system to allow inducible NFAT activation by stably transfecting the NKL-TAg cell line with the tetracyclin-sensitive transcriptional repressor (TetR) by hygromycin selection, allowing a doxycyclin (DOX)-on system in culture. Individual clones were tested by transient transfection with a luciferase reporter under control of two tetracycline operators (tetO). Stimulation with DOX for 24 hrs resulted in derepression of the reporter gene and over 100-fold activation of luciferase expression in four distinct TetR stable clones. Using two distinct TetR clones, a construct harboring an active form of NFAT under control of tetO operators was stably transfected in TetR cells using zeocin selection. Double stable clones were chosen using NFAT-reporter genes and western blots before and after DOX stimulation as selection criteria. Two double-stable TetR-NFAT clones were selected to control for potential cell based variations, AdCre infected to mortalize and adopt a cardiac muscle fate, and subjected to the Agilent microarray system and 44k mouse whole genome arrays. After DOX-stimulation for 24 hrs, 175 genes were differentially expressed in both clones with a 3 fold-change in expression. Gene ontology analysis revealed that NFAT target genes profoundly affect the cardiac transcriptome, signal transduction, translation efficiency and extracellular matrix. Conclusively, this novel cellular model allows for rapid genome wide screening of target genes of transcription factors in ventricular muscle, and will provide more entry points to our fundamental understanding of the calcineurin/NFAT transcriptional pathway in cardiac hypertrophy.

M. Bourajjaj, None; **A. Armand**, None; **R. Bassel-Duby**, None; **E.N. Olson**, None; **L.J. De Windt**, None.

P100

Differential Transcriptional Regulation of Cardiac Metabolic Genes by Myocyte Enhancer Factor-2 and Peroxisome Proliferator-Activated Receptors

Hamid el Azzouzi, Ralph J van Oort, Meriem Bourajjaj, Hubrecht Lab, Utrecht, The Netherlands; Marc van Bilsen, Cardiovascular Research Inst Maastricht, Maastricht, The Netherlands; Leon J De Windt, Hubrecht Lab, Utrecht, The Netherlands

During the progression to heart failure, changes in energy utilization occur in the heart, with the failing heart being more reliant on glucose utilization to the expense of fatty acid oxidation. Peroxisome proliferators-activated receptor (PPAR) family members are key regulators of cardiac fatty acid oxidation. In the regulatory region of the the PPAR target gene carnithine palmitoyl transferase-I (CPT-I), conserved PPAR response elements (PPRE) and myocyte enhancer factor-2 (MEF2) binding sites are present. We analyzed the transcriptional relationship between different PPAR isoforms (alpha, beta and gamma) and MEF2A by combinatorial site directed mutagenesis of the PPRE and MEF2 binding sites, and demonstrate a preferential relationship between PPARbeta and gamma with MEF2A, and that disruption of the PPRE increases activation of the CPT-I gene dramatically after stimulation with beta and gamma specific agonists. Furthermore, disruption of the MEF2 binding site completely abolished the activation of the reporter gene, irrespective whether the PPRE site was intact or not, suggesting that PPAR activity strongly depends on MEF2 transcriptional activity. Finally, a micro array analysis on cardiac muscle cell lines, which inducibly express a constitutively active form of MEF2, revealed that 20% of the differentially expressed genes were involved in mitochondrial metabolism/fatty acid oxidation. Remarkably, only a minority of these genes had PPRE sites and were responsive to PPAR agonists. Using RNAi-mediated downregulation of each PPAR isoform and a dominant negative MEF2 adenovirus, we confirmed the dominant role of MEF2 in the transcriptional regulation of endogenous metabolic genes. The combined observations suggest that for a select number of genes PPAR and MEF2 differentially converge to regulate adaptive fatty acid oxidation gene expression, with a dominant role for the bonafide pro-hypertrophic transcription factor MEF2. Further, MEF2 is also capable of altering the metabolic gene profile in cardiac muscle independent of PPAR activity. These data also suggest that the early hypertrophic phase is associated with an increased rather than decreased fatty acid utilization.

H. el Azzouzi, None; **R.J. van Oort**, None; **M. Bourajjaj**, None; **M. van Bilsen**, None; **L.J. De Windt**, None.

P101

Reduced-Energy Diet Improves the Survival of Viral Myocarditis in Obese Mice: Relation to Cardiac Adiponectin Expression

Tsugiyasu Kanda, Seiichiro Saegusa, Takashi Takahashi, Yu Fei, Shigeto Morimoto, Takeshi Nakahashi, Kunimitsu Iwai, Masayuki Matsumoto, Kanazawa Med Univ, Kahoku Ishikawa, Japan

Obesity is an important risk factor for heart diseases. Whether weight loss affects the extent of viral myocarditis is a matter of debate. We hypothesized that weight loss could improve cardiac function induced by cardiac expression of cardioprotective cytokine, adiponectin and reduction of cardiac TNF-alpha and also altered

immune reaction. We examined the relationship between weight loss and heart failure due to viral myocarditis in obese KKAy mice, comparing with wild type C57BL mice (WT). We intraperitoneally injected encephalomyocarditis virus (500 plaque-forming units/mouse) for KKAy feed ad libitum (100F) or 60% of the food intake (60F) and WT (n = 30 for each). Ten-day survival rate was 0% in 100F, whereas it was 17% in 60F and 40% in WT. Body weight in 60F was lower than in 100F (21.1 + 0.3 vs. 29.1 + 0.24 g, $P<0.05$, n = 4 for each) on Day 0 and continuously lower on Day 5. Heart weight/body weight ratio in 60F was lower than in 100F on Day 5 after viral inoculation (4.73 + 0.18 vs. 4.96 + 0.88 mg/g, $P<0.05$, n = 4 for each). Histological scores (0 to 5) for myocardial necrosis and inflammation on Day 5 were significantly lower in 60F than in 100F (necrosis; 1.8 + 0.3 vs. 3.2 + 0.7, $P<0.05$, inflammation; 1.4 + 0.5 vs. 2.2 + 0.4, $P<0.05$, $n_i = 4$ for each). Circulating adiponectin levels on Day 0 were significantly elevated in 60F compared with 100F (32 + 9 vs. 22 + 2 microg/mL, $P<0.05$) and those in 60F on Day 5 were also higher than in 100F. Comparative expression of cardiac adiponectin mRNA in 60F was significantly higher than in 100F (5.1 +0.3 vs. 1 + 0.2, $P<0.05$, n = 4 for each).and cardiac TNF-alpha mRNA in 60F were significantly decreased compared with in 100F on Day 5 (0.23 +0.03 vs. 1 + 0.3, $P<0.05$, n = 4 for each). Cardiac adiponectin mRNA was negatively correlated with cardiac TNF-alpha mRNA ($r=-0.53$, $P<0.01$, $n=12$). On Day 0, thymus weight/ body weight and spleen weight/body weight in 60F were significantly ($P<0.05$) lower than in 100F and WT. Weight loss improved the survival and myocardial damages in obese mice with viral myocarditis and also induced the cardiac expression of adiponectin. Therapeutic modulation of cardiac adiponectin might provide benefit to the cardioprotective effect against acute heart failure due to viral myocarditis in obese subjects.

T. Kanda, None; **S. Saegusa**, None; **T. Takahashi**, None; **Y. Fei**, None; **S. Morimoto**, None; **T. Nakahashi**, None; **K. Iwai**, None; **M. Matsumoto**, None.

P102

PPARα Activation Upregulates the Fatty Acid Oxidation Pathway and Reduces Cardiac Ceramide Content in Heart Failure but Does Not Affect LV Dysfunction

Margaret P Chandler, Eric E Morgan, Julie H Rennison, Tracy A McElfresh, Theodore A Kung, Case Western Reserve Univ, Cleveland, OH; Martin E Young, Univ of Texas Health Science Ctr, Houston, TX; Brian D Hoit, Univ Hosp of Cleveland, Cleveland, OH; William C Stanley, Case Western Reserve Univ, Cleveland, OH

Peroxisome proliferator activated receptor α (PPARα) overexpression in transgenic mice increases the lipotoxic intermediate ceramide and causes LV remodeling and dysfunction. Furthermore, in advanced heart failure (HF), the expression of genes regulated by PPARα is down-regulated causing decreased fatty acid oxidation (FAO), which may function as a positive compensatory response. We tested the hypothesis that up-regulation of the FAO pathway with a direct PPARα agonist would exacerbate left ventricular (LV) dysfunction and dilation in HF. Rats underwent left coronary artery ligation or sham surgery (n=10), and 8 weeks later were assigned treatment with the PPARα agonist fenofibrate (Inf+Feno, 150 $mg \cdot kg^{-1} \cdot day^{-1}$; n =13) or left untreated (Inf, n=10). Twenty weeks post ligation, LV function was assessed by echocardiography and catherization. LV systolic function was decreased and end diastolic area increased to a similar extent in both infarcted groups. Treatment with the PPARα-agonist up-regulated the mRNA expression of the PPARα regulated genes, and medium chain acyl-CoA dehydrogenase (MCAD) protein expression and activity were increased in the Inf+Feno group compared to sham and Inf groups (see Table). However, the mRNA and protein expression of PPARα and retinoid X receptor α were unchanged. Treatment with fenofibrate significantly increased LV mass/body mass ratio compared to sham and Inf groups. Although cardiac ceramide content was increased following infarction, PPARα activation reduced ceramide content. In conclusion, PPARα activation increased mRNA expression of FAO enzymes, increased MCAD protein expression and activity and reduced myocardial ceramide content. These results suggest that PPARα activation of the FAO pathway and ceramide content do not contribute to LV dysfunction and remodeling in a rat model of coronary artery ligation-induced HF.

LV Function, MCAD Activity & Tissue Ceramide in Sham, Inf and Inf+Feno Rats

	SHAM	INF	INF+FENO
LV End Diastolic Area (cm 2)	0.83 ± 0.08	1.21 ± 0.17	1.23 ± 0.09
Fractional Area of Shortening (%)	59 ± 2	28 ± 3	28 ± 4
MCAD Activity (umol/mg/min)	8.2 ± 0.5	7.8 ± 0.7	15.4 ± 1.0
Tissue Ceramide (nmol/g wet wt)	1.37 ± 0.07	1.99 ± 0.29	1.45 ± 0.08

M.P. Chandler, None; **E.E. Morgan**, None; **J.H. Rennison**, None; **T.A. McElfresh**, None; **T.A. Kung**, None; **M.E. Young**, None; **B.D. Hoit**, None; **W.C. Stanley**, None.

P103

Structural and Functional Changes in Heart Mitochondria from Sucrose-Fed Hypertriglyceridemic Rats

Karla Carvajal, Mohammed El Hafidi, Alvaro Marín-Hernández, Rafael Moreno-Sánchez, Inst Nacional de Cardiología, Mexico D.F., Mexico

In the heart of sugar-induced hypertriglyceridemic (HTG) rats, cardiac performance is impaired with glucose as fuel, but not with fatty acids. Accordingly, the glycolytic flux and the transfer of energy diminish in the HTG heart, in comparison to control heart. To further explore the biochemical nature of such alteration in the HTG heart, the components of the systems involved were evaluated. Total creatine kinase (CK) activity in the myocardial tissue was depressed by 30% in the HTG heart whereas the activity of mitochondrial CK (mitCK) isoenzyme decreased in isolated HTG heart mitochondria by 45%. Adenylate kinase (AK) was 20% lower in the HTG heart. In contrast, respiratory rates with 2-oxoglutarate (2-OG) and pyruvate/malate (pyr) were significantly higher in HTG heart mitochondria than in control mitochondria. 2-OG dehydrogenase activity was also higher in HTG mitochondria. Respiration with succinate was similar in both groups. Content of cytochromes b, c $+c_1$ and $a+a_3$, and cytochrome c oxidase activity, were also similar in the two kinds of mitochondria. A larger content of saturated and monounsaturated fatty acids was found in the HTG mitochondrial membranes with no changes in phospholipids composition or cholesterol content. Mitochondrial membranes from HTG hearts were more rigid, which correlated with the generation of higher electrochemical H^+ gradient across the inner mitochondrial membrane. As the mitochondrial function was preserved or even enhanced in the HTG heart, these results indicated that deficiency in energy transfer was mainly due to dysfunction in the mitCK and AK. This situation brought about uncoupling between the site of ATP production and the site of ATP consumption (contractile machinery), in spite of compensatory increase in mitochondrial oxidative capacity and H^+ gradient generation.

K. Carvajal, None; **M. El Hafidi**, None; **A. Marín-Hernández**, None; **R. Moreno-Sánchez**, None.

P104

Glucosamine-Induced Cardioprotection Mediated by the Hexosamine Biosynthesis Pathway and Increased Levels of O-Linked N-Acetylglucosamine on Nucleocytoplasmic Proteins

Norbert Fulop, Voraratt Champattanachai, Richard B Marchase, John C Chatham, Univ of Alabama at Birmingham, Birmingham, AL

Increased levels of O-linked N-acetylglucosamine (O-GlcNAc) on nucleocytoplasmic proteins are associated with decreased calcium entry into cardiomyocytes and improved tolerance of mammalian cells to stress. Therefore we tested the hypothesis that in the heart glucosamine (GlcN) treatment would increase hexosamine biosynthesis pathway (HBP) flux and protein O-GlcNAc levels, resulting in improved recovery following ischemia/reperfusion (I/R). In the isolated perfused rat heart the level of UDP-GlcNAc, a precursor for synthesis of O-GlcNAc was assessed by HPLC and protein O-GlcNAc levels were assessed by immunoblot analysis using CTD110, an anti O-GlcNAc antibody. Under normoxic conditions the addition of 5mM GlcN significantly increased UDP-GlcNAc levels from 72±7 to 126±7 nmols/g ($p<0.05$) and increased protein O-GlcNAc levels relative to untreated hearts (236±33% Vs 100±20%, $p<0.05$). Low flow ischemia (LFI, 0.3mls/min for 30min)

Available online at www.sciencedirect.com
SCIENCE DIRECT®
Life Sciences
Life Sciences 78 (2005) 195 – 204
www.elsevier.com/locate/lifescie

Inhibition of cyclooxygenase-2 enhances myocardial damage in a mouse model of viral myocarditis

Takashi Takahashi [a], Shi-jie Zhu [a], Hiroyuki Sumino [b], Seiichiro Saegusa [a], Takeshi Nakahashi [c], Kunimitsu Iwai [c], Shigeto Morimoto [c], Tsugiyasu Kanda [a,*]

[a] *Department of General Medicine, Kanazawa Medical University, 1-1 Daigaku, Uchinada-machi, Kahoku-gun, Ishikawa 920-0293, Japan*
[b] *Second Department of Internal Medicine, Gunma University School of Medicine, Gunma 371-8511, Japan*
[c] *Department of Geriatric Medicine, Kanazawa Medical University, Ishikawa 920-0293, Japan*

Received 27 October 2004; accepted 18 April 2005

Abstract

To determine critical role of cyclooxygenase-2 (COX-2) for development of viral myocarditis, a mouse model of encephalomyocarditis virus-induced myocarditis was used. The virus was intraperitoneally given to COX-2 gene-deficient heterozygote mice (*COX-2*$^{+/-}$) and wild-type mice (WT). We examined differences in heart weights, cardiac histological scores, numbers of infiltrating or apoptotic cells in myocardium, cardiac expression levels of COX-2, tumor necrosis factor-α (TNF-α), and adiponectin mRNA, immunoreactivity of COX-2, TNF-α, and adiponectin in myocytes, cardiac concentrations of TNF-α and adiponectin, prostaglandin E_2 (PGE_2) levels in hearts, and viral titers in tissues between *COX-2*$^{+/-}$ and WT. We observed significantly decreased expression of COX-2 mRNA and reactivity in hearts from *COX-2*$^{+/-}$ on day 8 after viral inoculation as compared with that from WT, together with elevated cardiac weights and severe inflammatory myocardial damage in *COX-2*$^{+/-}$. Cardiac expression of TNF-α mRNA, reactivity, and protein on day 8 was significantly higher in *COX-2*$^{+/-}$ than in WT, together with reciprocal expression of adiponectin mRNA, reactivity, and protein in hearts. Significantly reduced cardiac PGE_2 levels on day 8 were found in *COX-2*$^{+/-}$ compared with those in WT. There was no difference in local viral titers between both groups on day 4. Infected WT treated with a selective COX-2 inhibitor, NS-398, also showed the augmented myocardial damage on day 8. These results suggest that inhibition of COX-2 may enhance myocardial damage through reciprocal cardiac expression of TNF-α and adiponectin in a mouse model of viral myocarditis.

Keywords: Cyclooxygenase-2; Myocardial damage; Viral myocarditis; Prostaglandin E_2; Tumor necrosis factor-α; Adiponectin

Introduction

Cyclooxygenase (COX) catalyzes oxidation of arachidonic acid, producing prostaglandin (PG) H_2, which is then isomerized to biologically active eicosanoids and thromboxanes. Two distinct COX isoforms are identified: COX-1 is present in most cells and is constitutively expressed, whereas COX-2 is both inducible and the major isoform of inflammatory cells (DeWitt et al., 1993). COX-1 gene is more than 22 kb, and is located on chromosome arm 9q32–q33.3 in humans (Kosaka et al., 1994). The COX-2 gene is encoded by a gene more than 8 kb in size located on the long arm of chromosome 1q25.2–q25.3 (Kosaka et al., 1994). This gene is very similar to the mouse and chicken COX-2 genes (Kosaka et al., 1994). Mice with disrupted COX-1 or COX-2 genes have been generated using gene-targeting strategies (Langenbach et al., 1995; Morham et al., 1995), and the characteristics of these mice have been reviewed (Langenbach et al., 1999).

While a role of COX-1 in inflammation is largely unknown, COX-2 is likely to play a role in the inflammatory process and has been implicated as a mediator of various inflammatory diseases. Reduction of PG production by inhibition of COX is thought to be main mechanism of action of most non-steroidal anti-inflammatory drugs. It has also been described that COX-2-deficient mice are resistant to endotoxin-induced inflammation and death (Ejima et al., 2003). On the other hand, COX-2 deficiency has been reported to fail in altering inflammatory responses in several standard models (Dinchuk et al., 1995).

* Corresponding author. Tel.: +81 76 286 2211x3841; fax: +81 76 286 2702.
E-mail address: kandat@kanazawa-med.ac.jp (T. Kanda).

0024-3205/$ - see front matter © 2005 Elsevier Inc. All rights reserved.
doi:10.1016/j.lfs.2005.04.060

Viral infection, i.e. infection of encephalomyocarditis (EMC) virus is shown to stimulate COX-2 expression and PGE_2 accumulation through activation of nuclear factor-kappa B (NF-κB) in macrophages (Steer et al., 2003), and inhibitors of COX-2 enzymatic activity attenuate viral replication (Chen et al., 2000; Zhu et al., 2002), suggesting that the expression of COX-2 and the increased production of PG may possess an important role in viral replication. COX-2 enzyme is also described to be protective against pulmonary fibrogenesis, indicating that COX-2 generation of PGE_2 is a critical factor in resolving inflammation (Bonner et al., 2002).

COX-2 is reported to be up-regulated in an animal model of cardiac failure (Adderley and Fitzgerald, 1999), and its induction and activation of NF-κB has been detected in cardiomyocytes of patients with congestive heart failure (Wong et al., 1998). Deletion of the COX-2 gene may result in myocardial fibrosis (Dinchuk et al., 1995). Several manuscripts suggest that COX-2 plays a crucial role in mediating cardioprotective effects of ischemic preconditioning, which is the most potent anti-ischemic intervention known to date in terms of endogenous protection of ischemic myocardium (Shinmura et al., 2000; Bolli et al., 2002), since PGE_1 of COX-2 metabolites exerts cardioprotective action such as reduction in infarct size (Simpson et al., 1988).

We hypothesized that endogenous cardiac expression of COX-2 could play a cardioprotective role in establishment of severe inflammatory conditions induced by EMC virus. Therefore, we determined degrees of myocardial damage in the COX-2-deficient mice with acute viral myocarditis based on the histopathological findings and cardiac expression of tumor necrosis factor-alpha (TNF-α) mRNA, immunoreactivity, and protein in comparison with those in the wild-type mice with myocarditis.

Materials and methods

Animals

B6;129S7-*Ptgs2*^{tm1Jed} (*COX-2*$^{+/-}$) mice and C57BL/6 wild-type (WT) mice (3–5 weeks old) were purchased from the Jackson Laboratory (Bar Harbor, Maine, USA) as described previously (Yokota et al., 2002). High mortality and unavailability precluded use of homozygous *COX-2*$^{-/-}$ animals in this experiment.

Virus

A myocarditic variant of EMC virus was obtained from Y. Seto, Ph.D. (Keio University, Tokyo, Japan). Virus preparations were stored at −80 °C in Eagle's minimum essential medium (MEM) supplemented with 0.1% fetal bovine serum until the time of use.

Infection protocol

Animals were intraperitoneally inoculated with 500 plaque-forming units of EMC virus suspended in 0.1 ml of saline.

Treatment protocol

We administered EMC virus to WT ($n=12$) and *COX-2*$^{+/-}$ ($n=12$) mice. A normal WT mouse without viral inoculation was also included. Cardiac tissues were immediately extracted after sacrifice by cervical dislocation in both groups on days 4 and 8 after the EMC virus inoculation.

Histological examinations of hearts

Hearts were immediately weighed after sacrifice. Body weights were also recorded before sacrifice. Ratios of heart weight to body weight were calculated in both groups. Halves of cardiac tissues were fixed in 10% buffered formalin and stained with hematoxylin–eosin (H&E), while the other halves were immediately frozen in liquid nitrogen and stored at −80 °C for the studies of COX-2, PGE_2, and cytokine. Two transverse sections of the ventricular myocardium were graded for the severity of necrosis and mononuclear cell infiltration by an experienced pathologist, who had no knowledge of our study design, according to the following scale: grade 1, lesions involving <25% of the ventricular myocardium; grade 2, lesions involving 25% to 50% of the myocardium; grade 3, lesions involving 50% to 75% of the myocardium; and grade 4, lesions involving >75% of the myocardium. We also performed the staining on myosin as well as the H&E staining to identify the myocyte necrosis accurately. In addition, the pathologist randomly selected five high power fields (HPF) (×400 magnification) from each transverse section of the myocardium, and counted the infiltrating cells. The number of apoptotic cells in the randomly selected 5 HPF (×400 magnification) per section in the transverse sections of the myocardium was determined with in situ TUNEL as previously described (Kanda et al., 1999).

Comparative expression levels of COX-2, TNF-α, and adiponectin mRNA in hearts

RNA extraction for each half of frozen cardiac tissues was performed as described by the manufacturer (RNeasy Mini Kit, QIAGEN Inc., Tokyo, Japan). Procedure of DNAase was performed during the RNA extraction to avoid DNA contaminations. The total RNA concentrations were determined by measuring the optical density at 260 and 280 nm. Aliquots of 20 μl RNA from the each tissue were applied for production of cDNA. Comparative expression levels of COX-2, TNF-α, and adiponectin mRNA in cardiac tissues from both groups were determined using a quantitative real-time reverse transcriptase–polymerase chain reaction (RT–PCR) as described previously (Takeda et al., 2004). We applied TaqMan MGB Probe (Applied Biosystems Inc., CA, USA) for the real-time PCR. Primers and probe for quantification of COX-2 transcript (synthesized by Hokkaido System Science Co. Ltd., Hokkaido, Japan) were designed using a primer design software Primer Express (Applied Biosystems Inc.). We used a commercially available kit for TNF-α and

adiponectin RT-PCR (Mm00443258 m1 and Mm00456425 m1, Applied Biosystems Inc.). Each threshold cycle number up to 50 cycles (C_t value) within the RT–PCR was examined for the COX-2, TNF-α, and adiponectin mRNA levels. Glyceraldehyde-3-phosphate dehydrogenase (GAPDH) gene was used as an endogenous internal standard, and was amplified with specific primers for the number of cycles. A negative control without template cDNA was always included. ΔC_t values referred to differences between the C_t values for the each target gene and the GAPDH gene. After confirming that efficiencies of amplification of the each molecule and GAPDH transcripts were approximately equal, amount of the COX-2, TNF-α, or adiponectin transcript relative to the GAPDH transcript was determined using the comparative C_t method described in Perkin Elmer Applied Biosystems User Bulletin #2 (1997). Data are expressed as fold-increases relative to the baseline values in heart from a normal WT mouse without viral inoculation.

Immunoreactivity of COX-2, TNF-α, and adiponectin in cardiomyocytes

Immunohistochemical staining by streptavidin biotin complex method (#K0675 and #E0466 or #E0353, DAKO Cytomation Co. Ltd., Kyoto, Japan) was performed for the sections of transverse ventricular myocardium obtained from both groups on days 4 and 8 after viral infection. As a normal control, the immunoreactivity of COX-2, TNF-α, and adiponectin was determined with heart from a normal WT mouse without viral inoculation. We used the following commercially available primary antibodies; goat polyclonal anti-mouse COX-2 antibody at dilution of 1:100 (#sc-1747, Santa Cruz Biotechnology Inc., CA, USA), goat polyclonal anti-mouse TNF-α antibody at dilution of 1:50 (#RC410, DAKO Cytomation Co. Ltd.), and rabbit polyclonal anti-mouse adiponectin antibody at dilution of 1:50 (#ACRP303-A, Alpha Diagnostic International Inc., TX, USA). Control slides were treated with normal diluted goat or rabbit serum. The slides were blindly reviewed by the same pathologist, and were semiquantitatively graded according to the positive degrees of immunoreactivity as 0 for absence of staining and 1+ for weak, 2+ for moderate, and 3+ for strong staining (Kanazawa et al., 1996). They were compared with the respective control slides to exclude nonspecific staining. The positive degrees of COX-2, TNF-α, and adiponectin reactivity were assessed for randomly selected 30 myocytes corresponding to the surviving cells found on the respective H&E and myosin-stained slides.

Cardiac levels of TNF-α and adiponectin

Partial remnants of frozen cardiac tissues were applied to measurement of TNF-α and adiponectin tissue levels with the homogenate of each tissue. Enzyme-linked immunosorbent assay (ELISA) method, which used a polyclonal antibody specific for mouse TNF-α or adiponectin pre-coated onto a microtiter plate (ELISA kit for TNF-α; BioSource International Inc., CA, USA) (ELISA kit for adiponectin; Otsuka Pharmaceutical Co., Ltd., Tokyo, Japan), was performed with cardiac samples according to the instructions of manufactures. As a normal control, cardiac levels of TNF-α and adiponectin were determined with heart from a normal WT mouse without viral infection. The ELISA kit applied for TNF-α concentrations showed that the limit of sensitivity and the within- and between-assay variations were 3.0 pg/ml, 6.5%, and 8.7%, respectively. The kit used for adiponectin levels demonstrated that the limit of sensitivity, the intra-assay variation, and the cross-reactivity were 0.25 ng/ml, less than 10%, and no responses for specimens from other animals including sheep, respectively.

Concentrations of PGE2 in hearts

Partial remnants of frozen cardiac samples from both groups on day 8 after viral infection were applied to measurement of PGE_2 tissue levels with the homogenate of each tissue as described previously (LaPointe et al., 2004). We also examined PGE_2 concentration with heart from a normal WT mouse without viral inoculation. Radioimmunoassay (RIA) method was performed using a commercially available kit with the tissue samples according to the instructions of manufactures (Prostaglandin E_2 [^{125}I] RIA Kit, Perkin Elmer Life Sciences Inc., MA, USA). This RIA kit used for plasma PGE_2 levels demonstrated that the sensitivity limit and the intra- and inter-assay variations were 0.5 pg/ml, 9.0–9.4%, and 6.7–11.6%, respectively.

Viral titers in hearts

EMC viral titers in hearts were determined in terms of the viral cytopathic effects, and were expressed as the tissue culture mean infectious dose ($TCID_{50}$). On day 4 after the inoculation ($n=6$ for each group), hearts were partially

Table 1
Body weight, cardiac weight, and ratio of cardiac weight to body weight in different mice groups after viral inoculation

	Body weight (g)			Cardiac weight (mg)		Ratio of cardiac weight to body weight	
	Day 0	Day 4	Day 8	Day 4	Day 8	Day 4	Day 8
WT	19.3±1.1	18.9±1.9	17.9±2.3	98±8	102±11	5.3±0.4	5.8±0.7
COX-2$^{+/-}$	19.5±1.6	19.0±2.2	16.2±2.5	102±10	116±13*	5.5±0.5	7.2±0.9*
NS-398	19.9±1.3	19.2±1.8	16.8±2.8	104±13	127±19*	5.6±0.7	7.5±1.1*

WT, wild-type mice; *COX-2*$^{+/-}$, mice with heterozygous deficiency of cyclooxygenase-2 gene; NS-398, wild-type mice treated with a selective inhibitor of cyclooxygenase-2, NS-398, at a dose of 3 mg/kg/day starting simultaneously with viral inoculation. Data are expressed as means±S.D.
* $P<0.05$ compared with WT mice group.

homogenized in 2 ml of MEM. After centrifugation, the supernatants were added into 96-well microtiter plates containing human amnion cells in MEM supplemented with 10% fetal calf serum as described previously (Kanda et al., 2000). The microtiter plates were observed daily for 5 days for the appearance of any cytopathic effects.

Reassessment study by a selective COX-2 inhibitor

In order to confirm the augmented myocardial damage, we orally administered WT mice ($n=12$) a selective COX-2 inhibitor, NS-398 (EMD Biosciences Inc., Darmstadt, Germany), at dosing of 3 mg/kg/day starting simultaneously with

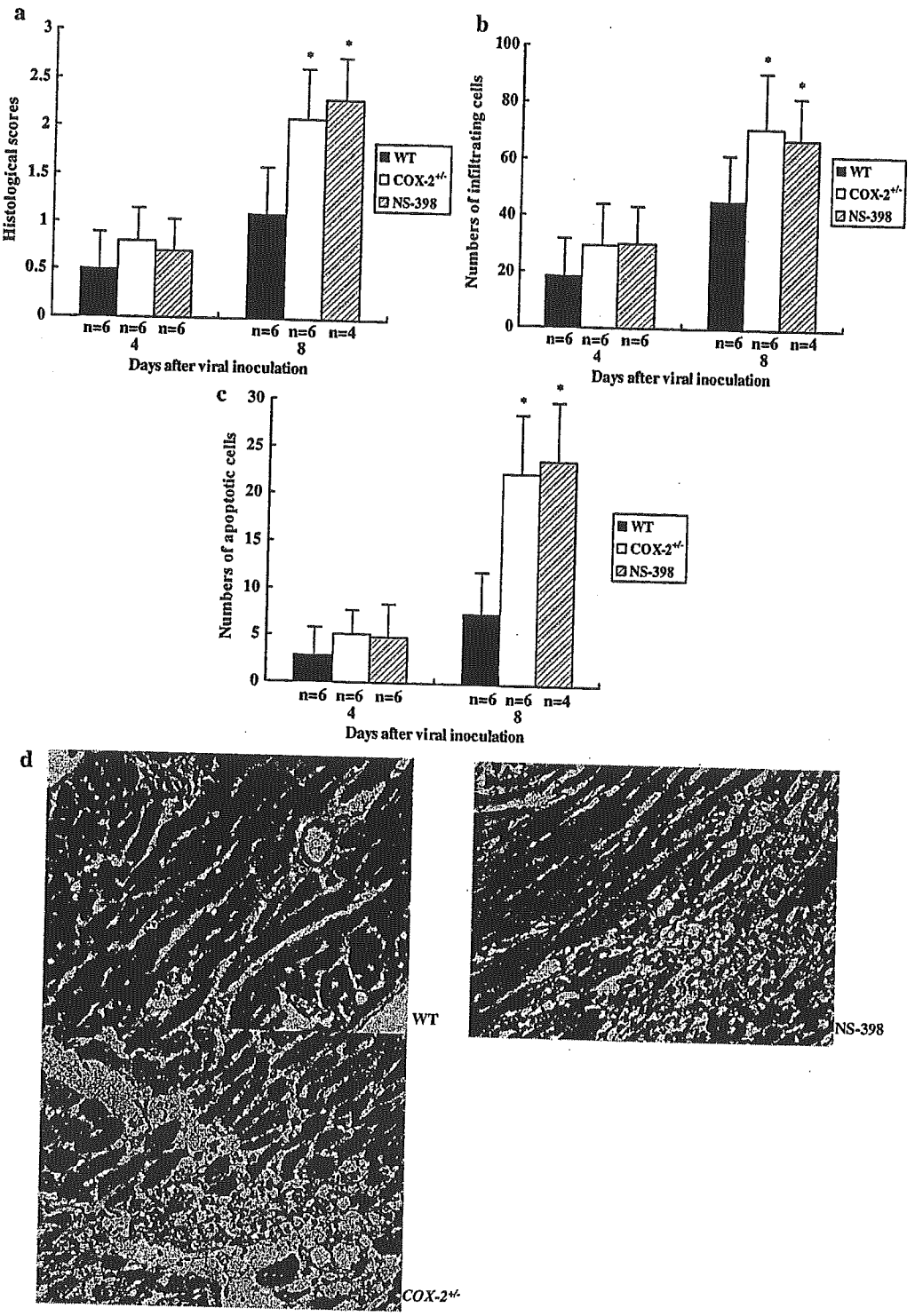

Fig. 1. Results of histological examination including histological scores in heart (a), numbers of infiltrating cells (b) or apoptotic cells (c) in myocardium from different mice on days 4 and 8 after viral inoculation, and photographic demonstration of myocardial damage in three groups on day 8 (d, original magnification). Data are expressed as mean±S.D. WT, wild-type mice; *COX-2*$^{+/-}$, mice with heterozygous deficiency of cyclooxygenase-2 gene; NS-398, wild-type mice treated with a selective inhibitor of cyclooxygenase-2, NS-398, at a dose of 3 mg/kg/day starting simultaneously with viral inoculation. *$P<0.05$ compared with the WT group.

viral inoculation as described previously (LaPointe et al., 2004). Histological examinations (cardiac histological scores and numbers of infiltrating or apoptotic cells in myocardium), as well as body weights, heart weights, and ratios of heart weight to body weight, were assessed with hearts obtained on days 4 and 8 after viral infection. Data were compared with those in infected WT mice without intervention of the COX-2 inhibitor.

Statistical analysis

Data are expressed as mean±standard deviations. A two-tailed analysis of variance was applied to evaluate differences in body and cardiac weights, ratios of heart weight to body weight, cardiac histological scores, numbers of infiltrating or apoptotic cells in myocardium among three groups. An unpaired two-tailed Student's *t*-test was used to assess differences in comparative expression levels of COX-2, TNF-α, and adiponectin mRNA in hearts, immunoreactivity of COX-2, TNF-α, and adiponectin in myocytes, cardiac levels of TNF-α and adiponectin, PGE_2 concentrations in hearts, and local EMC viral titers between the *COX-2*$^{+/-}$ mice and the WT mice. A value of $P<0.05$ was considered to be statistically significant.

Results

Mortality in different mice with viral myocarditis

There were no dead mice with viral myocarditis in the WT group and the *COX-2*$^{+/-}$ group. Numbers of mice in each group from which specimens of hearts were obtained on days 4 and 8 after EMC viral inoculation, were 6 on each day in the WT mice and 6 on each day in the *COX-2*$^{+/-}$ mice, respectively.

Body weights, cardiac weights, and ratios of cardiac weight to body weight

Body weights, heart weights, and ratios of heart weight to body weight in different groups are shown in Table 1. Cardiac weights in the *COX-2*$^{+/-}$ group on day 8 after viral infection were significantly increased as compared with those in the WT group ($P<0.05$, Table 1). There was also significant difference in ratios of cardiac weight to body weight between the *COX-2*$^{+/-}$ mice and the WT mice on day 8 ($P<0.05$, Table 1).

Histological findings in hearts

Histological scores and numbers of infiltrating or apoptotic cells per field in the hearts obtained from different mice on days 4 and 8 after viral inoculation are shown in Fig. 1a, b, and c, respectively. The hearts from the *COX-2*$^{+/-}$ group showed severe myocardial necrosis and mononuclear cell infiltration (Fig. 1d). The histological scores based on myocardial necrosis and cell infiltration on day 8 were significantly higher in the *COX-2*$^{+/-}$ mice than in the WT mice ($P<0.05$, Fig. 1a). The number of infiltrating cells per field in the myocardium from the *COX-2*$^{+/-}$ group on day 8

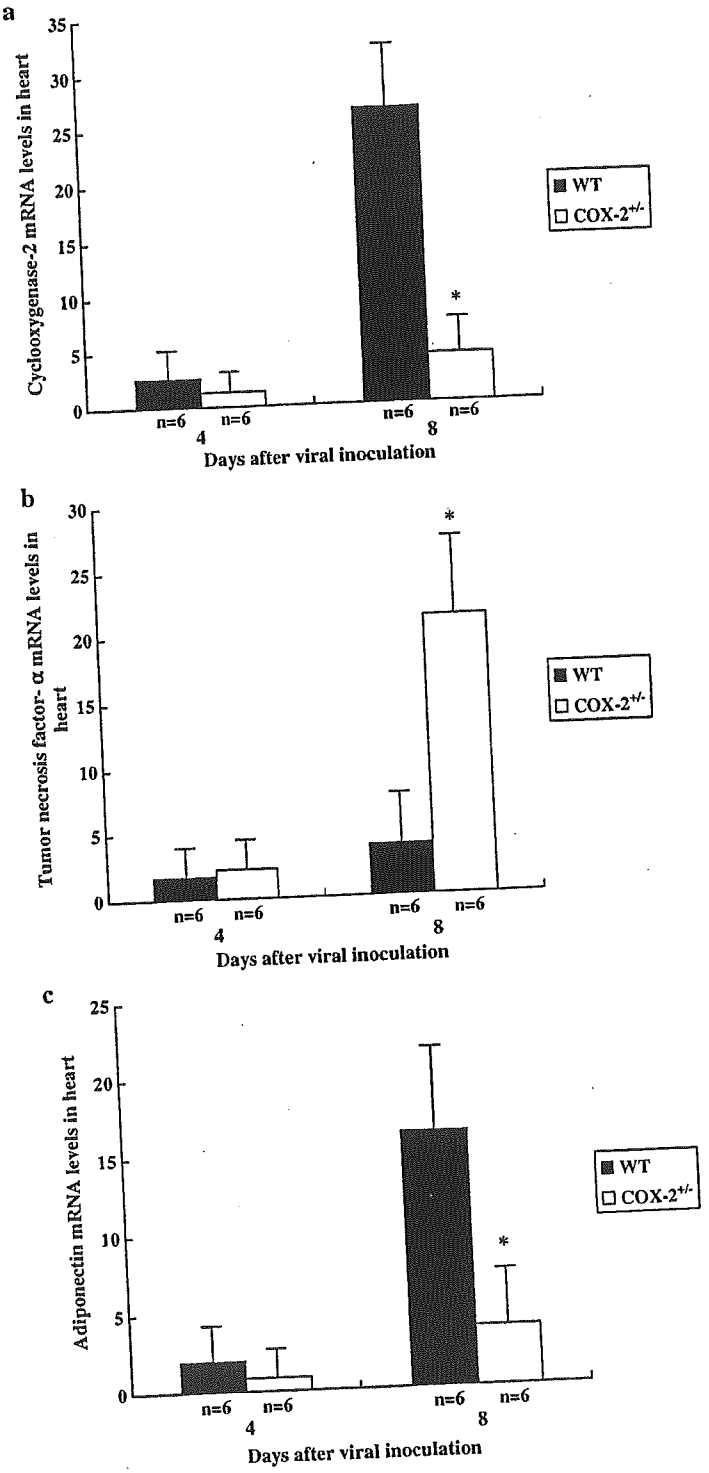

Fig. 2. Results of comparative expression levels of cyclooxygenase-2 (a), tumor necrosis factor-α (b), and adiponectin (c) mRNA using a quantitative real-time reverse transcriptase–polymerase chain reaction with hearts from different mice on days 4 and 8 after viral infection. Data are expressed as mean±S.D. WT, wild-type mice; *COX-2*$^{+/-}$, mice with heterozygous deficiency of cyclooxygenase-2 gene; COX-2, cyclooxygenase-2; TNF-α, tumor necrosis factor-α. *$P<0.05$ compared with the WT group.

was significantly elevated as compared with that in the WT group ($P<0.05$, Fig. 1b). The number of apoptotic cells per field in the hearts on day 8 was significantly higher in the *COX-2*$^{+/-}$ mice than in the WT mice ($P<0.05$, Fig. 1c). There were no significant differences in histological scores and numbers of infiltrating or apoptotic cells between the *COX-2*$^{+/-}$ group and the WT group on day 4.

Comparative expression levels of COX-2, TNF-α, and adiponectin mRNA in hearts

Tissue sample of heart from a normal WT mouse was assigned to each value of 1 for tissue expression levels of COX-2, TNF-α, and adiponectin mRNA, respectively. Cardiac levels of COX-2, TNF-α, and adiponectin mRNA from

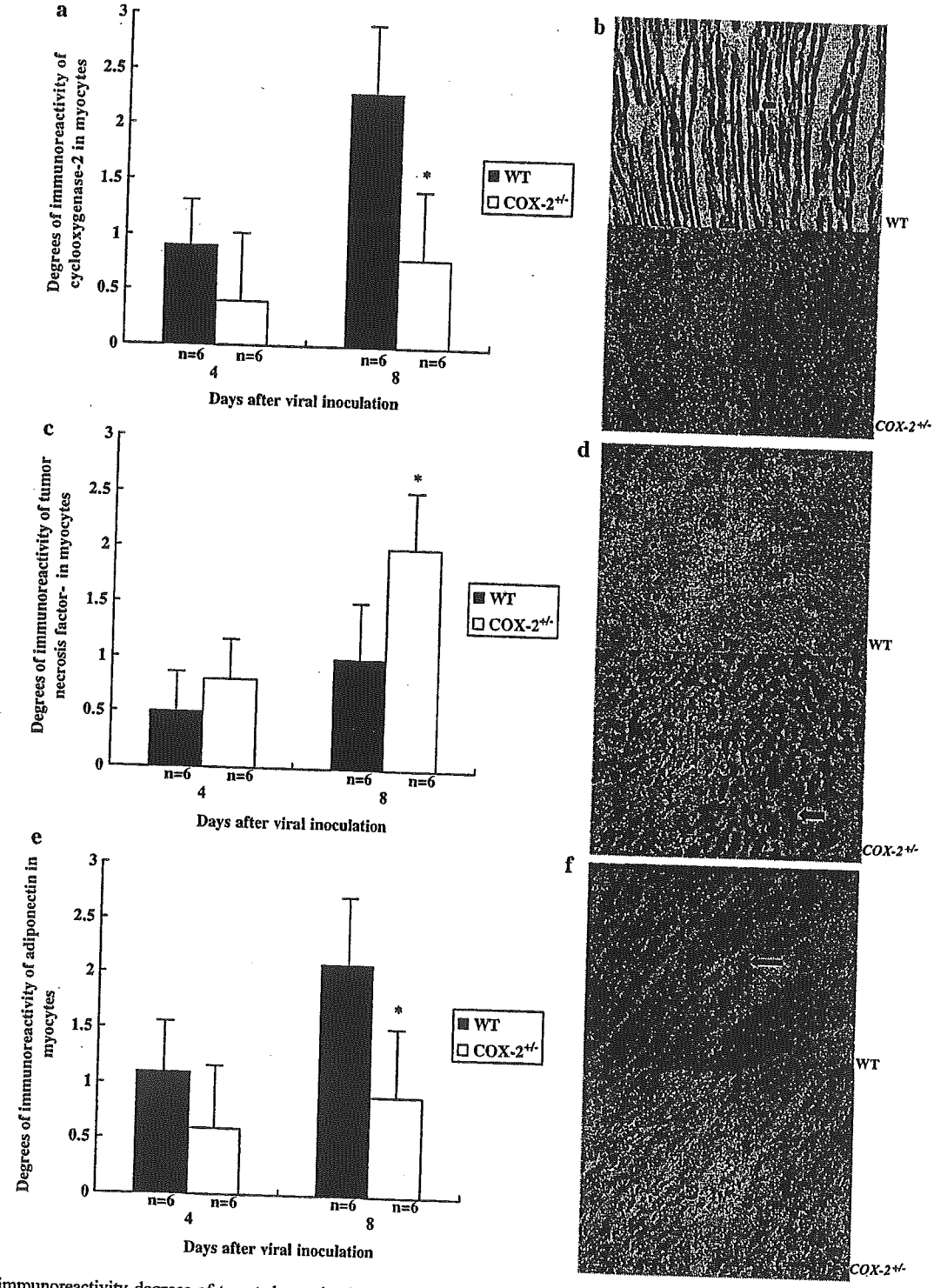

Fig. 3. Results of immunoreactivity degrees of targeted proteins including cyclooxygenase-2 (a), tumor necrosis factor-α (c), adiponectin (e) in myocytes from different mice on days 4 and 8 after viral inoculation, and photographic demonstration (arrows) of cyclooxygenase-2 (b, original magnification), tumor necrosis factor-α (d, original magnification), and adiponectin (f, original magnification) reactivity in myocardium from various mice on day 8. Data are expressed as mean±S.D. WT, wild-type mice; *COX-2*$^{+/-}$, mice with heterozygous deficiency of cyclooxygenase-2 gene. *$P<0.05$ compared with the WT group.

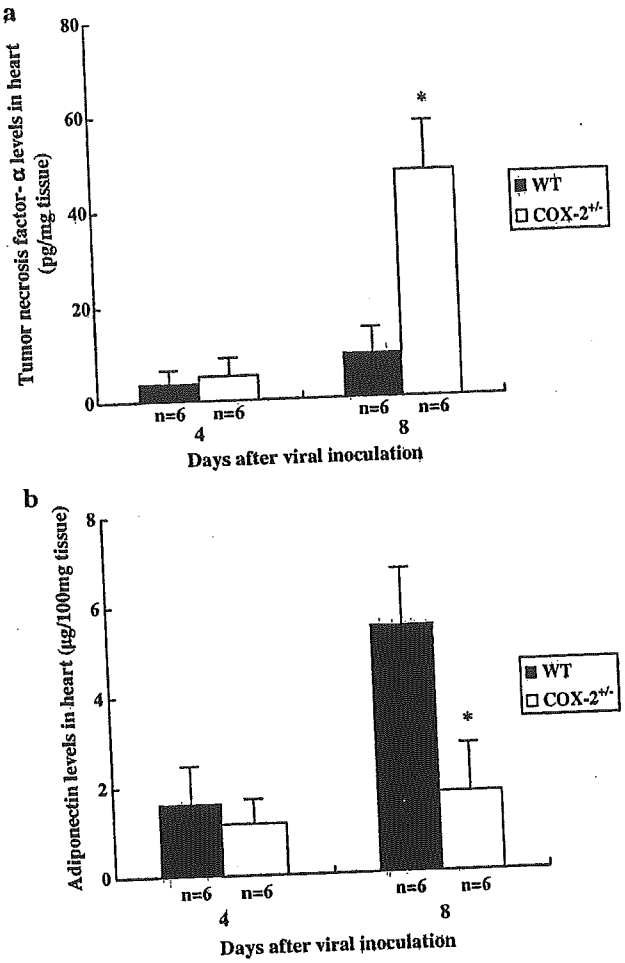

Fig. 4. Results of tumor necrosis factor-α (a) and adiponectin (b) levels in hearts from different mice on days 4 and 8 after viral inoculation. Data are expressed as mean±S.D. WT, wild-type mice; *COX-2*$^{+/-}$, mice with heterozygous deficiency of cyclooxygenase-2 gene. *$P<0.05$ compared with the WT group.

different mice on days 4 and 8 after viral infection are shown in Fig. 2a, b, and c, respectively. COX-2 mRNA levels in hearts on day 8 were significantly lower in the *COX-2*$^{+/-}$ group than in the WT group ($P<0.05$, Fig. 2a). On the other hand, we observed the significantly increased levels of TNF-α mRNA in cardiac tissues from the *COX-2*$^{+/-}$ mice at the same time as compared with those from the WT mice ($P<0.05$, Fig. 2b). Adiponectin mRNA levels in hearts on day 8 were significantly suppressed in the *COX-2*$^{+/-}$ group than in the WT group ($P<0.05$, Fig. 2c). There was no difference in cardiac levels of COX-2, TNF-α, and adiponectin mRNA between the WT mice and the *COX-2*$^{+/-}$ mice on day 4.

Immunoreactivity of COX-2, TNF-α, and adiponectin in cardiomyocytes

Immunoreactivity of COX-2, TNF-α, and adiponectin was not observed in heart from a normal WT mouse. The degrees of COX-2, TNF-α, and adiponectin reactivity in damaged myocytes from different mice on days 4 and 8 after viral inoculation are shown in Fig. 3a, c, and e, respectively. Photographic demonstration of immunoreactivity of COX-2, TNF-α, and adiponectin in cardiac tissues from various mice on day 8 is indicated in Fig. 3b, d, and f, respectively. We found the significantly suppressed reactivity of COX-2 in myocytes from the *COX-2*$^{+/-}$ group on day 8 as compared with that from the WT group ($P<0.05$, Fig. 3a and b). On the other hand, the degrees of TNF-α reactivity in myocytes at the same time were significantly higher in the *COX-2*$^{+/-}$ mice than in the WT mice ($P<0.05$, Fig. 3c and d). The degrees of adiponectin reactivity in myocytes on day 8 were significantly decreased in the *COX-2*$^{+/-}$ group than in the WT group ($P<0.05$, Fig. 3e and f). There were no differences in degrees of COX-2, TNF-α, and adiponectin reactivity between the WT mice and the *COX-2*$^{+/-}$ mice on day 4.

Cardiac levels of TNF-α and adiponectin

Specimen of heart from a normal WT mouse showed undetectable values for each targeted molecule. TNF-α and adiponectin levels in hearts from different mice on days 4 and 8 after viral infection are shown in Fig. 4a and b, respectively. Cardiac concentrations of TNF-α on day 8 were significantly higher in the *COX-2*$^{+/-}$ mice than in the WT mice ($P<0.05$, Fig. 4a). On the other hand, there were significantly reduced adiponectin levels in hearts from the *COX-2*$^{+/-}$ group at the same time as compared with those from the WT group ($P<0.05$, Fig. 4b). There were no differences in cardiac concentrations of TNF-α and adiponectin between the *COX-2*$^{+/-}$ mice and WT mice on day 4.

Concentrations of PGE2 in hearts

Tissue specimen of heart obtained from a normal WT mouse showed 0.96 pg/mg protein. Cardiac PGE_2 concentrations from different mice on day 8 after viral infection are shown in Fig. 5. The PGE_2 tissue levels on day 8 were significantly lower in the *COX-2*$^{+/-}$ mice than in the WT mice ($P<0.05$, Fig. 5).

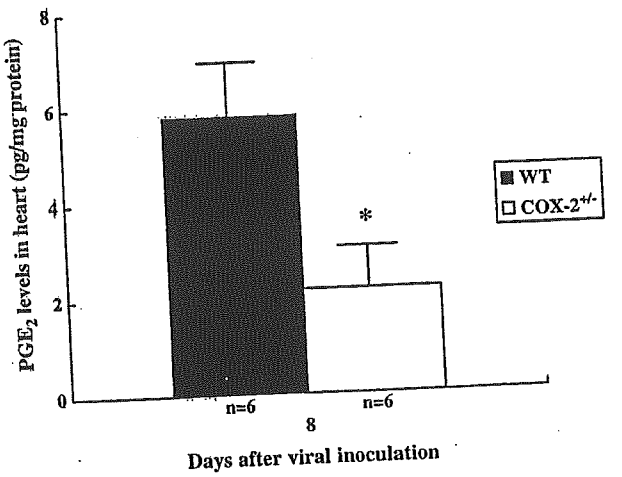

Fig. 5. Results of cardiac prostaglandin E_2 concentrations from different mice on day 8 after viral inoculation. Data are expressed as mean±S.D. WT, wild-type mice; *COX-2*$^{+/-}$, mice with heterozygous deficiency of cyclooxygenase-2 gene. *$P<0.05$ compared with the WT group.

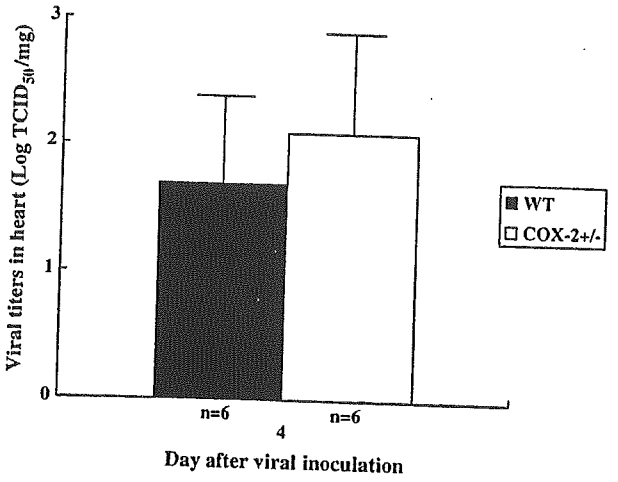

Fig. 6. Results of encephalomyocarditis viral titer in hearts from different mice on day 4 after viral infection. Data are expressed as mean±S.D. WT, wild-type mice; *COX-2*$^{+/-}$, mice with heterozygous deficiency of cyclooxygenase-2 gene; $TCID_{50}$, tissue culture mean infectious dose 50%.

Viral titers in hearts

EMC viral titers in hearts from various mice on day 4 after viral inoculation are indicated in Fig. 6. There was no difference in local viral titers between the *COX-2*$^{+/-}$ mice and the WT mice on day 4 after viral inoculation.

Reassessment study by a selective COX-2 inhibitor

We observed two dead WT mice treated with NS-398 on day 8 after viral infection. The numbers of mice from which hearts were extracted on days 4 and 8 were six and four, respectively. Cardiac weights and ratios of heart weight to body weight in the NS-398 group on day 8 were significantly increased compared to those in the WT group ($P<0.05$, Table 1). The histological scores and numbers of infiltrating or apoptotic cells in myocardium on day 8 were significantly higher in the WT mice treated with NS-398 than in the WT mice without intervention ($P<0.05$, Fig. 1a, b, and c). The augmented myocardial damage in the WT mice treated with NS-398 is shown in Fig. 1d. There were no differences in the histological scores and numbers of infiltrating or apoptotic cells between the NS-398 group and the WT group on day 4.

Discussion

The fold-increase of COX-2 mRNA expression in *COX-2*$^{+/-}$ mice compared to that in sham-infected animal was "one-seventh fold" less than the fold-increase in WT mice on day 8 after viral inoculation. Cardiac PGE_2 levels on day 8 were about one-third suppressed in the *COX-2*$^{+/-}$ group compared to those in the WT group. EMC virus infection has recently been reported to stimulate COX-2 expression in macrophages in in vitro experiment (Steer et al., 2003). Another study showed no expression of COX-2 mRNA in *COX-2*$^{-/-}$ primary embryonic fibroblasts and less expression of mRNA in *COX-2*$^{+/-}$ fibroblasts under stimulation (Dinchuk et al., 1995). Thus, decreased expression of COX-2 mRNA in hearts from *COX-2*$^{+/-}$ mice with viral infection seems to be due to the disruption of one COX-2 allele.

COX-2 products can exhibit both beneficial and deleterious effects on inflammatory process in the same organ such as the kidney (Wang et al., 2000). COX-2 expression is also described to protect against apoptosis in several types of cells, particularly in colon cancer cells (Kinoshita et al., 1999). Myocardial COX-2 expression is demonstrated in rat heart during cardiac transplant rejection (Yang et al., 2000), and COX activity induced by doxorubicin in rat neonatal cardiomyocytes is due to COX-2 gene expression (Hemler and Lands, 1976). It has recently been reported that COX-2 expression may provide some degrees of protective effects against the myocardial damage in the rat model of doxorubicin-induced cardiotoxicity (Dowd et al., 2001). On the other hand, COX-2 is indicated to play a deleterious role in heart after myocardial infarction caused by chronic occlusion of left anterior descending coronary artery (LaPointe et al., 2004). COX-2 inhibition partly reverses both the increase in cardiac collagen content and hypertrophy and the decrease in cardiac function in the mouse model of myocardial infarction. Similarly to the findings in the former manuscript, we observed impaired expression of cardiac COX-2 resulted in augmented myocardial injury in *COX-2*$^{+/-}$ mice with EMC virus-induced myocarditis as compared with that in WT mice. Since the inoculation of EMC virus promotes COX-2 expression and PGE_2 generation (Steer et al., 2003), the up-regulation of COX-2 expression is considered to play a crucial role for compensatory mechanism in the mouse model of heart failure induced by EMC virus infection.

TNF-α mRNA is shown to be detectable in myocardium obtained from subjects with ischemic heart disease (IHD) and dilated cardiomyopathy (DCM) using northern blot analysis, while there is no evidence for TNF-α gene expression in non-failing human hearts (Torre-Amione et al., 1996). Immunohistochemical examinations also indicated that there was obvious TNF-α immunostaining of cardiomyocytes in the myocardium from patients with IHD and DCM, whereas the TNF-α immunoreactivity was not detectable in the non-failing hearts (Torre-Amione et al., 1996). Natriuretic peptides including atrial and B-type peptides are synthesized in and secreted from hearts, and play a critical role in cardiovascular homeostasis (Grepin et al., 1994). Similarly to the previous demonstration, identification of TNF-α expression in hearts from mice with viral myocarditis in our study is also a good example of contribution made by molecular biology to understanding of mechanisms for heart failure compensation.

Prostaglandins acts on 2 classes of receptors consisting of surface transmembrane-spanning, G-protein-coupled receptors and peroxisome proliferator-activated receptors (PPARs), which are nuclear membrane receptors. Prostaglandins and their precursors are ligands for several PPARs including PPARα, PPARδ, and PPARγ (Bishop-Bailey and Hla, 1999). PPARγ activates transcription level of adiponectin with liver receptor homologue-1 by binding the promoter region of

adiponectin gene (Ouchi et al., 2004). Cardiac expression of adiponectin was impaired together with decreased PGE_2 concentrations in hearts from *COX-2*$^{+/-}$ mice with viral myocarditis. Reactivity of adiponectin for immunostaining has recently been reported to be observed at periphery of surviving cardiomyocytes around the lesions at granulative stage in myocardial tissues obtained from 47 autopsied hearts with infarction (Ishikawa et al., 2003). In another immunohistochemical analysis, boundary of mouse hepatocytes showed positive signals for adiponectin after 3–6 h of carbon tetrachloride treatment, and their cytoplasma was intensely stained after 18 h of the treatment (Yoda-Murakami et al., 2001). Adiponectin was considered to be produced by the liver in mice, where it underwent tissue damage-induced transcriptional regulation (Yoda-Murakami et al., 2001). Our data regarding adiponectin expression in damaged myocytes suggest that this adipocyte-specific cytokine might have important implications for acute phase of viral myocarditis.

Adiponectin is described to be involved in ending inflammatory responses through its inhibitory functions (Yokota et al., 2000). This cytokine increases mRNA expression of anti-inflammatory molecule, interleukin-10 (IL-10), at the transcriptional level, and elevates IL-10 protein secretion in in vitro experiment of human monocyte-derived macrophages (Kumada et al., 2004). In addition, reciprocal relationship between adiponectin and high-sensitive C-reactive protein is shown in both human plasma and adipose tissue from subjects with coronary artery disease (Ouchi et al., 2003). In our experiment, suppressed expression of cardiac adiponectin mRNA and immunoreactivity in *COX-2*$^{+/-}$ mice was associated with the development of severe myocarditis, whereas increased expression of adiponectin in hearts from WT mice resulted in the inhibition of cardiac inflammatory process. Therefore, we speculate that local expression of adiponectin in the damaged myocardium might be a compensatory phenomenon against the severe inflammatory conditions of viral myocarditis.

A COX-2 inhibitor, Dup-697, suppressed the biological action of adiponectin on differentiation of cloned stromal preadipocytes (Yokota et al., 2002). Adiponectin was described to inhibit TNF-α production in macrophages (Yokota et al., 2000). Adiponectin-knockout mice revealed high levels of TNF-α mRNA in adipose tissue and high plasma TNF-α concentrations (Maeda et al., 2002). Thus, impaired COX-2 functions seem to link to increased cardiac expression of TNF-α mRNA, immunoreactivity, and protein through the reduced expression of adiponectin mRNA, reactivity, and protein in our experiment.

In conclusion, decreased expression of COX-2 mRNA and immunoreactivity in myocardium from *COX-2*$^{+/-}$ mice after viral infection were observed together with increased heart weights, severe myocardial inflammation, and suppressed cardiac PGE_2 concentrations in *COX-2*$^{+/-}$ mice. There was also an enhanced expression of TNF-α mRNA, reactivity, and protein in hearts, while attenuated cardiac expression of adiponectin mRNA, reactivity, and protein was found in *COX-2*$^{+/-}$ mice with viral myocarditis. Moreover, infected WT mice treated with the selective COX-2 inhibitor showed the augmented myocardial damage on day 8. Our observations suggest that inhibition of COX-2 and subsequent reduced PGE_2 production in heart may contribute to enhanced myocardial injury through reciprocal cardiac expression of TNF-α and adiponectin in a mouse model of viral myocarditis.

Acknowledgment

This study was supported in part by Grant for Promoted Research from Kanazawa Medical University (S2003-2 and S2004-2), Grant for Project Research from High-Technology Center of Kanazawa Medical University (H2004-7), and the Science Research Promotion Fund of the Promotion and Mutual Aid Corporation for Private Schools of Japan.

References

Adderley, S.R., Fitzgerald, D.J., 1999. Oxidative damage of cardiomyocytes is limited by extracellular regulated kinases 1/2-mediated induction of cyclooxygenase-2. Journal of Biological Chemistry 274 (8), 5038–5046.

Bishop-Bailey, D., Hla, T., 1999. Endothelial cell apoptosis induced by the peroxisome proliferator-activated receptor (PPAR) ligand 15-deoxy-Delta12, 14-prostaglandin J2. Journal of Biological Chemistry 274 (24), 17042–17048.

Bolli, R., Shinmura, K., Tang, X.L., Kodani, E., Xuan, Y.T., Guo, Y., Dawn, B., 2002. Discovery of a new function of cyclooxygenase (COX)-2: COX-2 is a cardioprotective protein that alleviates ischemia/reperfusion injury and mediates the late phase of preconditioning. Cardiovascular Research 55 (3), 506–519.

Bonner, J.C., Rice, A.B., Ingram, J.L., Moomaw, C.R., Nyska, A., Bradbury, A., Sessoms, A.R., Chulada, P.C., Morgan, D.L., Zeldin, D.C., Langenbach, R., 2002. Susceptibility of cyclooxygenase-2-deficient mice to pulmonary fibrogenesis. American Journal of Pathology 161 (2), 459–470.

Chen, N., Warner, J.L., Reiss, C.S., 2000. NSAID treatment suppresses VSV propagation in mouse CNS. Virology 276 (1), 44–51.

DeWitt, D.L., Meade, E.A., Smith, W.L., 1993. PGH synthase isoenzyme selectivity: the potential for safer nonsteroidal antiinflammatory drugs. American Journal of Medicine 95 (2A), 40S–44S.

Dinchuk, J.E., Car, B.D., Focht, R.J., Johnston, J.J., Jaffee, B.D., Covington, M.B., Contel, N.R., Eng, V.M., Collins, R.J., Czerniak, P.M., Gorry, S.A., Trzaskos, J.M., 1995. Renal abnormalities and an altered inflammatory response in mice lacking cyclooxygenase II. Nature 378 (6555), 406–409.

Dowd, N.P., Scully, M., Adderley, S.R., Cunningham, A.J., Fitzgerald, D.J., 2001. Inhibition of cyclooxygenase-2 aggravates doxorubicin-mediated cardiac injury in vivo. Journal of Clinical Investigation 108 (4), 585–590.

Ejima, K., Layne, M.D., Carvajal, I.M., Kritek, P.A., Baron, R.M., Chen, Y-H., Vom Saal, J., Levy, B.D., Yet, S.F., Perrella, M.A., 2003. Cyclooxygenase-2-deficient mice are resistant to endotoxin-induced inflammation and death. FASEB Journal 17 (10), 1325–1327.

Grepin, C., Dagnino, L., Robitaille, L., Haberstroh, L., Antakly, T., Nemer, M., 1994. A hormone-encoding gene identifies a pathway for cardiac but not skeletal muscle gene transcription. Molecular and Cellular Biology 14 (5), 3115–3129.

Hemler, M., Lands, W.E., 1976. Purification of the cyclooxygenase that forms prostaglandins. Demonstration of two forms of iron in the holoenzyme. Journal of Biological Chemistry 251 (18), 5575–5579.

Ishikawa, Y., Akasaka, Y., Ishii, T., Yoda-Murakami, M., Choi-Miura, N.H., Tomita, M., Ito, K., Zhang, L., Akishima, Y., Ishihara, M., Muramatsu, M., Taniyama, M., 2003. Changes in the distribution pattern of gelatin-binding protein of 28 kDa (adiponectin) in myocardial remodelling after ischaemic injury. Histopathology 42 (1), 43–52.

Kanazawa, K., Kawashima, S., Mikami, S., Miwa, Y., Hirata, K., Suematsu, M., Hayashi, Y., Itoh, H., Yokoyama, M., 1996. Endothelial constitutive nitric oxide synthase protein and mRNA increased in rabbit atherosclerotic aorta